

Stationary and Oscillatory Spatial Patterns Induced by Global Periodic Switching

J. Buceta,¹ Katja Lindenberg,¹ and J. M. R. Parrondo²

¹*Department of Chemistry and Biochemistry and Institute for Nonlinear Science, University of California–San Diego, 9500 Gilman Drive, La Jolla, California 92093-0340*

²*Departamento de Física Atómica, Molecular y Nuclear, Universidad Complutense de Madrid, Ciudad Universitaria s/n, 28040 Madrid, Spain*

(Received 7 September 2001; published 26 December 2001)

We propose a new mechanism for pattern formation based on the global alternation of two dynamics, neither of which exhibits patterns. When driven by either one of the separate dynamics, the system goes to a spatially homogeneous state associated with that dynamics. However, when the two dynamics are globally alternated sufficiently rapidly, the system exhibits stationary spatial patterns. Somewhat slower switching leads to oscillatory patterns. We support our findings by numerical simulations and discuss the results in terms of the symmetries of the system and the ratio of two relevant characteristic times, the switching period and the relaxation time to a homogeneous state in each separate dynamics.

DOI: 10.1103/PhysRevLett.88.024103

PACS numbers: 47.54.+r, 05.45.–a, 89.75.Kd

Patterns in nonequilibrium systems arise in a variety of ways. For example, so-called dissipative structures arise from perturbations of homogeneous systems if the input of energy is properly balanced by dissipation [1]. Perhaps the best-known dissipative structure is the Bénard instability, formed when a layer of liquid is heated from below. At a given temperature, heat conduction starts to occur predominantly through convection, and regularly spaced, hexagonal convection cells are formed in the layer of liquid. This structure is present only as long as there is a supply of heat and disappears when this ceases. Many other examples involve chemical oscillations in dissipative open systems [1]. Patterns may also form by the temporal modulation of a parameter in systems that undergo Hopf bifurcations. This modulation may stabilize standing waves or wave patterns that are otherwise unstable for any constant value of the parameter in this regime [2,3]. A different sort of phenomenon, that of noise-induced pattern formation, may occur when an external spatially and temporally uncorrelated noise affects a system parameter. The parameter fluctuations may induce spatial organization and pattern formation in a system where only a homogeneous state is stable when the parameter is constant [4,5].

In this Letter we identify and illustrate a new mechanism for pattern formation induced by a global periodic alternation between two dynamics, each of which by itself leads to a (different) spatially homogeneous state. This mechanism is inspired by a number of examples where simple periodic switching between two dynamics, each of which produces “uninteresting” or “disordered” or even “undesirable” states, leads to an “interesting” or “ordered” or “desirable” outcome. One example is the flashing Brownian ratchet, a rectifier of thermal fluctuations that can induce directed motion of Brownian particles merely by turning the ratchet potential on and off periodically [6]. Another (in turn inspired by the ratchet example) is that of so-called paradoxical games, where the alternation of two losing games may lead to a winning game [7]. Our pro-

posed mechanism applies these ideas to spatially extended systems.

We focus on a class of model systems based on the Swift-Hohenberg (SH) equation [8]:

$$\dot{\varphi}(\mathbf{r}, t) = -V'(\varphi(\mathbf{r}, t)) + \mathcal{L}\varphi(\mathbf{r}, t) + \xi(\mathbf{r}, t), \quad (1)$$

where the operator $\mathcal{L} = -(1 + \nabla^2)^2$ is a spatial coupling, and the white zero-centered Gaussian noise $\xi(\mathbf{r}, t)$ with correlation $\langle \xi(\mathbf{r}, t)\xi(\mathbf{r}', t') \rangle = \sigma^2 \delta(t - t')\delta(\mathbf{r} - \mathbf{r}')$ accounts for thermal or other fluctuations. The dynamics of the system is determined by the local potential $V(\varphi)$, which in the standard SH model is an even quartic function of φ . The SH model leads to pattern formation (e.g., to the appearance of Rayleigh-Bénard convective rolls) when the local potential has two stable equilibrium points. However, if $V(\varphi)$ is *monostable*, no spatial structures appear in this system and the steady state is spatially homogeneous. The stability boundary is identified by determining a uniform solution of the (noiseless) evolution equation (1) and linearizing about this solution. The stationarity condition $V'(\varphi) + \varphi = 0$ (the term φ arises from the 1 in the coupling operator) has the solution $\varphi \equiv \tilde{\varphi}$. Setting $\varphi = \tilde{\varphi} + \Delta\varphi$ gives for the Fourier transform (denoted by a hat) of the linearized equation

$$\Delta \dot{\hat{\varphi}}(\mathbf{k}, t) = -[V''(\tilde{\varphi}) + (1 - |\mathbf{k}|^2)^2]\Delta \hat{\varphi}(\mathbf{k}, t), \quad (2)$$

and if $V''(\tilde{\varphi}) < 0$ a morphological instability first sets in for the modes with $|\mathbf{k}| = 1$. Note that in the usual SH model the even local potential leads to $\tilde{\varphi} = 0$ and that in general the patterns that emerge depend on the symmetry of the potential. Thus, symmetry of the evolution equation under the $\varphi \leftrightarrow -\varphi$ inversion leads to roll-shaped patterns, while absence of this symmetry leads to hexagonally arranged spotlike structures [9].

Consider now a *global* periodic switching of period T between two local potentials, V_1 and V_2 . Thus, *every* point is subject to the same local potential at any given time. The system is governed by the equation

$$\dot{\varphi}(\mathbf{r}, t) = -V'_+(\varphi(\mathbf{r}, t)) - \mu(t)V'_-(\varphi(\mathbf{r}, t)) + \mathcal{L}\varphi(\mathbf{r}, t) + \xi(\mathbf{r}, t), \quad (3)$$

where $V_{\pm}(\varphi) \equiv [V_1(\varphi) \pm V_2(\varphi)]/2$ and $\mu(t)$ takes on the value 1 if $t \bmod T < T/2$ and -1 if $t \bmod T > T/2$. The resulting equation is a SH model with dichotomous periodic external forcing. To the best of our knowledge, this forcing differs from those previously considered in the literature [2].

In order to investigate whether the switching mechanism can lead to pattern formation, we focus on local potentials $V_1(\varphi)$ and $V_2(\varphi)$ that satisfy the stability conditions,

$$V'_i(\tilde{\varphi}_i) + \tilde{\varphi}_i = 0 \quad \text{and} \quad V''_i(\tilde{\varphi}_i) > 0 \quad (4)$$

(monostable potentials), whereas their average $V_+(\varphi)$ does not. Note that the condition that $V_+(\varphi)$ *not* satisfy (4) implies that both local potentials cannot be quadratic. As a consequence, for the proposed pattern formation mechanism nonlinearity is a necessary component.

When each potential acts separately, the system tends to a homogeneous state. The expectation of pattern formation when the potentials are periodically alternated arises as follows. If the switching period T is large, every point in the system has time to equilibrate to the local potential before the local potentials switch. Regardless of the initial distribution, the entire system is expected to oscillate with period T between the homogeneous states corresponding to each potential. On the other hand, if T is sufficiently small (see below), $\mu(t)$ can be adiabatically eliminated and replaced by its average value, which is zero. The system is then driven by the potential $V_+(\varphi)$, for which there is at least one state $\tilde{\varphi}$ with

$$V'_+(\tilde{\varphi}) + \tilde{\varphi} = 0 \quad \text{and} \quad V''_+(\tilde{\varphi}) < 0, \quad (5)$$

and thus patterns appropriate to this local potential are expected to occur. Away from these extremes, the behavior depends on the switching rate. More specifically, the crossover time t_r between slow and fast switching is the smaller of $t_{1 \rightarrow 2}$ and $t_{2 \rightarrow 1}$, where $t_{i \rightarrow j}$ is the relaxation time, *under the action of* V_j , of the homogeneous state associated with V_i . We can estimate $t_{i \rightarrow j}$ by focusing only on the $\mathbf{k} = 0$ mode and assuming that, when the potential switches from V_i to V_j , the mode amplitude behaves as a Brownian particle initially equilibrated in the effective local potential $\tilde{V}_i(\varphi) = V_i(\varphi) + \frac{\varphi^2}{2}$. When the local potential is switched, this point, which up to that moment was stable, becomes unstable. The relaxation time to the new homogeneous state associated with V_j is the time that it takes the Brownian particle to roll down the potential hill to the new equilibrium point [10]:

$$t_{i \rightarrow j} = \frac{2}{\sigma^2} \int_{\tilde{\varphi}_i}^{\tilde{\varphi}_j} dy \exp\left(\frac{2}{\sigma^2} \tilde{V}_j(y)\right) \times \int_{\tilde{\varphi}_i}^y dz \exp\left(-\frac{2}{\sigma^2} \tilde{V}_j(z)\right). \quad (6)$$

The behavior of the system (3) can be characterized by the ratio of the time $T/2$ that the system spends in each dynamics to the crossover time t_r , $r \equiv T/2t_r$.

Let us focus on a particular choice of potentials satisfying the conditions (4) and (5):

$$V_{1,2}(\varphi) = A_{1,2} \left(\frac{\varphi^4}{4} \pm \frac{\varphi^3}{3} - \frac{\varphi^2}{2} \mp \varphi \right), \quad (7)$$

where $A_{1,2}$ are positive constants. The corresponding effective local potentials with $A_1 = A_2 = 1$ are shown in Fig. 1. The average potential is

$$V_+(\varphi) = a_+ \frac{\varphi^4}{4} + a_- \frac{\varphi^3}{3} - a_+ \frac{\varphi^2}{2} - a_- \varphi, \quad (8)$$

where $a_{\pm} = (A_1 \pm A_2)/2$. If $r \gg 1$ the entire system alternates between the homogeneous states $\tilde{\varphi}_{1,2}$. When $r \lesssim 1$, we expect pattern formation with outcomes dependent on the specific value of r and on the equality or inequality of the parameters $A_{1,2}$. We support our reasoning with $2d$ numerical simulations of a discretized form of Eq. (3) with these potentials, periodic boundary conditions, and parameters $L_x = L_y = 64$, $\sigma = 10^{-2}$ (the fluctuations must be sufficiently small not to swamp the potential barrier in V_+). Since the most unstable mode is $|\mathbf{k}^*| \approx 1$ [5], the typical wavelength of any pattern is expected to be $\lambda = 2\pi/|\mathbf{k}^*| \approx 2\pi$ and the aspect ratio $L/\lambda \sim 10$. In our simulations we take either the initial field to be random according to a Gaussian distribution (in which case the additive fluctuations can actually be omitted entirely) or we can take an arbitrary initial condition (e.g., all points equilibrated with V_1), in which case the fluctuations will distribute the field in any case. In some cases we choose an initial configuration that facilitates arrival at a particular final state simply to avoid

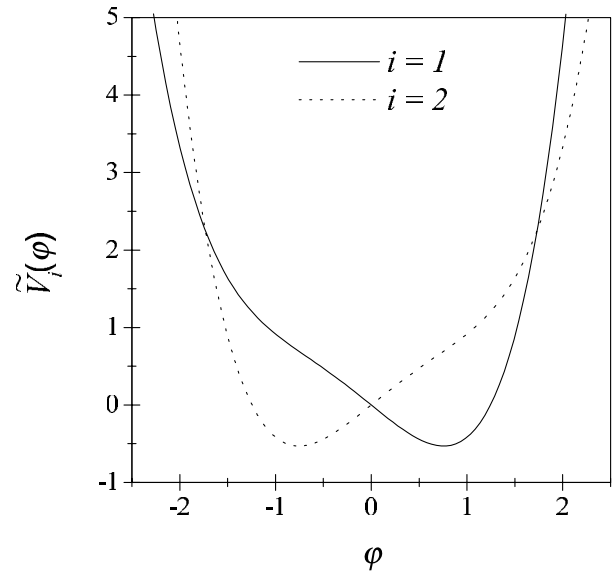


FIG. 1. Effective local potentials $\tilde{V}_1(\varphi)$ (solid curve) and $\tilde{V}_2(\varphi)$ (dotted curve) with $A_1 = A_2 = 1$. The mirror symmetry is broken if $A_1 \neq A_2$.

a very long simulation time. At the initial time every local potential is set to, say, V_1 , at time $T/2$ all the potentials are switched to V_2 , and so on.

If $A_1 = A_2$, $V_+(\varphi)$ is an even function and, in the limit $r \rightarrow 0$, Eq. (3) satisfies inversion symmetry under the transformation $\varphi \leftrightarrow -\varphi$. In this case we expect the appearance of *stationary rolls* [9]. This is clearly seen in Fig. 2. Note that the widths of the rolls are consistent with the aspect ratio given earlier. On an extremely long time scale, as in the SH model, the rolls line up in a more ordered fashion.

As r increases toward the “resonance” condition $r \approx 1$, the contribution of $V'_-(\varphi)$ can no longer be neglected. Hence Eq. (3) will lack the symmetry $\varphi \leftrightarrow -\varphi$, and an *oscillatory* spotlike pattern is expected [9]. Furthermore, with $A_1 = A_2$, Eq. (3) is invariant under the combined transformation $\{\varphi \leftrightarrow -\varphi, \mu \leftrightarrow -\mu\}$, which requires a *square* spatial arrangement of the oscillatory pattern [9]. A realization is shown in Fig. 3, for which $t_r = t_{1 \rightarrow 2} = t_{2 \rightarrow 1} \approx 2$. The resonant period of the forcing is $T \approx 4$. We show color encoded snapshots of the field, where the oscillatory square patterns are clearly visible. Note that the field oscillates between a square lattice and its glide-transformed one. In other words, the spot centers do not move or oscillate; it is the surrounding background that oscillates. We are able to reproduce this behavior analytically through a decomposition in a small number of modes [11]. The size of the pattern units is again consistent with the aspect ratio given earlier. The oscillatory pattern and the lattice arrangement of the spots resemble the so-called *oscillons* found in vibrating granular media and clay [12].

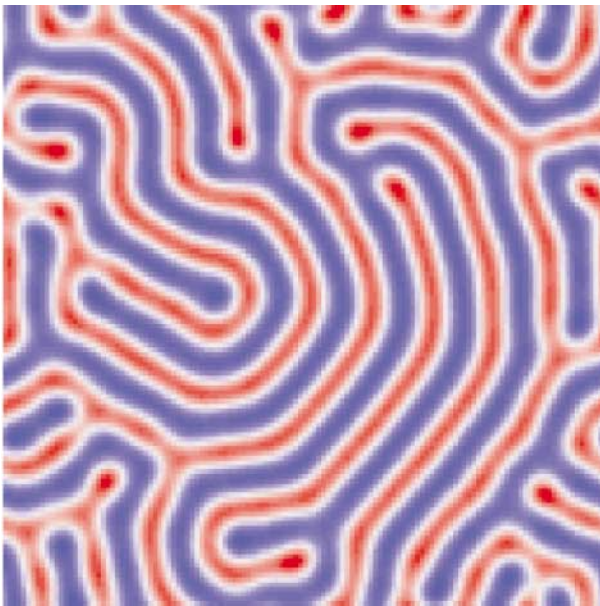


FIG. 2 (color). Density plot of the field for the case $A_1 = A_2 = 1$ and $r = 0.25$. The roll-shaped pattern is essentially (see text) stationary.

The behavior is in some ways simpler when $A_1 \neq A_2$. The inversion symmetry $\varphi \leftrightarrow -\varphi$ is no longer satisfied. Therefore, both stationary ($r \ll 1$) and dynamic ($r \approx 1$) hexagonal spot patterns are expected [9]. We have simulated the case $A_1 = 1$, $A_2 = 2$, for which the relaxation time is calculated to be $t_r \approx 1.6$. As always, if $r \gg 1$ no spatial structures develop; homogeneous states simply alternate in time. On the other hand, for $r = 0.94$, we again obtain oscillatory patterns, as shown in the snapshots of Fig. 4. It is worth noting that this excitation density is quite different from the one in Fig. 3. As expected, the spots are arranged hexagonally. Most strikingly, in this case there is no glide oscillation but rather a true oscillation of localized excitations whose size is again consistent with the calculated aspect ratio. As r is decreased the excitation field

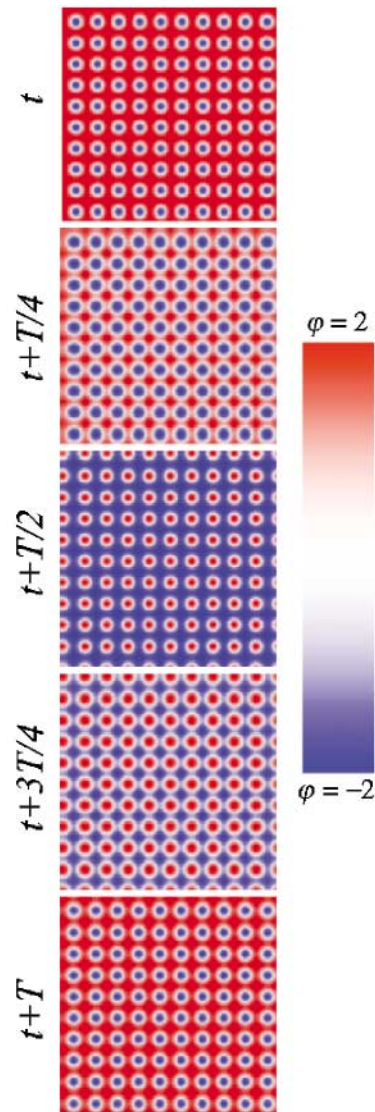


FIG. 3 (color). Snapshots of the field during a full period of the dichotomous forcing ($A_1 = A_2 = 1$ and $r = 1.15$). Note the oscillations of the field between the square lattice and its glide-transformed one.

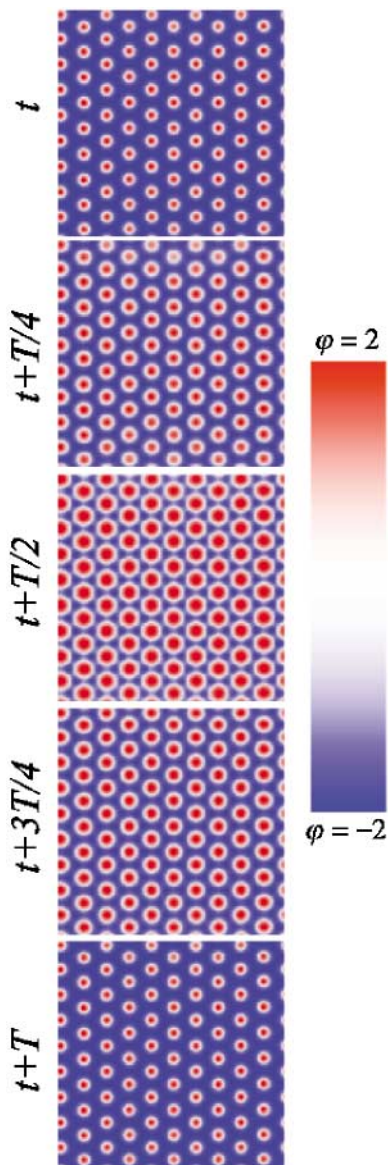


FIG. 4 (color). Snapshots of the field for the case $A_1 = 1$, $A_2 = 2$, and $r = 0.94$ during a full period of the forcing function. The localized excitations are arranged in a hexagonal lattice.

is frozen and one obtains a stationary hexagonal pattern of spots.

We have also performed simulations of Eq. (3) when the modulation $\mu(t)$ is a dichotomous noise. In this case, the intermediate regime of oscillatory patterns fades out and the system exhibits alternating homogeneous states if the correlation time of $\mu(t)$ is large and stable patterns (rolls or hexagons) if the correlation time is small [11].

Summarizing, we have shown that the alternation of two dynamics can create patterns even though each separate dynamics drives the system to a homogeneous state. Moreover, we have seen that in the crossover between alternating homogeneous states and stationary patterns, a rich

phenomenology of oscillatory patterns may emerge. The mechanism is very general and can easily be extended to other situations such as reaction-diffusion systems. Thus, we have provided an alternative nonequilibrium mechanism to dissipative structures or modulation of bifurcation parameters for the formation of stationary and oscillatory spatial patterns.

An interesting open problem is whether it is possible to find this type of behavior when the switching occurs between two equilibrium dynamics. This is not the case in the SH equation, even when the homogeneous state is stable. For instance, in the case of convection, the homogeneous state describes a fluid in mechanical but not in thermal equilibrium. If switching between local potential is achievable in the case of convection, our results would imply that the system will exhibit convection patterns by alternating dynamics which separately drive the fluid to mechanical (but not to thermal) equilibrium.

The authors thank R. Kawai for fruitful discussions. This work was partially supported by the National Science Foundation under Grant No. PHY-9970699, by DGES-Spain Grant No. PB-97-0076, by the *New Del Amo Program*, and by MEC-Spain Grant No. EX2001-02880680.

-
- [1] P. Manneville, *Dissipative Structures and Weak Turbulence* (Academic, Boston, 1990); H. Mori and Y. Kuramoto, *Dissipative Structures and Chaos* (Springer, Berlin, 1998).
 - [2] C. W. Meyer, D. S. Cannell, G. Ahlers, J. B. Swift, and P. C. Hohenberg, *Phys. Rev. Lett.* **61**, 947 (1988); D. Walgraef, *J. Stat. Phys.* **64**, 969 (1991).
 - [3] C. Careta and F. Sagués, *J. Chem. Phys.* **92**, 1098 (1990); F. Drolet and J. Viñals, *Phys. Rev. E* **56**, 2649 (1997).
 - [4] J. García-Ojalvo and J. M. Sancho, *Noise in Spatially Extended Systems* (Springer, New York, 1999); C. Van den Broeck, J. M. R. Parrondo, R. Toral, and R. Kawai, *Phys. Rev. E* **55**, 4084 (1997).
 - [5] J. M. R. Parrondo, C. Van den Broeck, J. Buceta, and F. J. de la Rubia, *Physica (Amsterdam)* **224A**, 153 (1996).
 - [6] A. Ajdari and J. Prost, *C. R. Acad. Sci., Ser. II* **315**, 1635 (1992); R. D. Astumian and M. Bier, *Phys. Rev. Lett.* **72**, 1766 (1994).
 - [7] G. P. Harmer and D. Abbott, *Stat. Sci.* **14**, 206 (1999); *Nature (London)* **402**, 864 (1999); J. M. R. Parrondo, G. P. Harmer, and D. Abbott, *Phys. Rev. Lett.* **85**, 5226 (2000).
 - [8] J. Swift and P. C. Hohenberg, *Phys. Rev. A* **15**, 319 (1977).
 - [9] M. C. Cross and P. C. Hohenberg, *Rev. Mod. Phys.* **65**, 851 (1993).
 - [10] C. W. Gardiner, *Handbook of Stochastic Methods* (Springer, Berlin, 1985), 2nd ed.; A. N. Malakhov, *Chaos* **7**, 488 (1997).
 - [11] J. Buceta, J. M. R. Parrondo, and K. Lindenberg (to be published).
 - [12] P. B. Umbanhowar, F. Melo, and H. L. Swinney, *Nature (London)* **382**, 793 (1996).